View metadata, citation and similar papers at core.ac.uk
brought to you by CORE
provided by DSpace at VSB Technical University of Ostrava

Tm-Yb Doped Optical Fiber Performance with Variation of Host-Glass Composition

Anirban DHAR, Atasi PAL, Shyamal DAS, Ranjan SEN

Fiber Optics & Photonics Division, CSIR-Central Glass & Ceramic Research Institute, 196 Raja. S. C. Mullick Road, Jadavpur, Kolkata-700 032, West-Bengal, India

anirband@cgcri.res.in, atasi@cgcri.res.in, dshyamal@cgcri.res.in, rsen@cgcri.res.in

Abstract. *The fabrication process of Thulium-Ytterbium doped optical fiber comprising different host glass through the Modified Chemical Vapor Deposition (MCVD) coupled with solution doping technique is presented. The material and optical performance of different fibers are compared with special emphasis on their lasing efficiency for 2 μm application.*

Keywords

Amplified spontaneous emission, laser performance, MCVD-solution process, Thulium-Ytterbium doped fiber.

1. Introduction

Presently, Ytterbium doped high-power fiber laser has reached the power level in kW range and research is aiming to enhance the power level further beside increasing long-term stability by optimizing fiber fabrication process (fiber design and host material) with sophisticated instrumentation. Thulium (Tm) doped fiber laser is another important research topic due to their potential application in the eye-safe 2 μm region that have significant potential for a variety of medical and biosensor applications [3], [4], [5]. Tm ion in silica glass matrix exhibits several energy levels and among several possible transitions $^3F_4$ to $^3H^6$ transition is the most important for near infra-red (NIR) application which can be achieved through excitation at around 0.8 μm, 1.2 μm and 1.6 μm. In order to use available laser diode for pumping purpose, co-doping of Ytterbium (Yb) in Tm-fiber is well known. Accordingly, doping of Thulium-Ytterbium in an appropriate glass host enables to explore the possibility of pumping over the wavelength region from 0.91 to 0.98 μm for emission in the range of 2 μm. However, proper selection of host glass composition which alters glass phonon energy and tunes the spectral properties are essential to improve fiber performance for practical application.

The sensitization of Tm^{3+} by Yb^{3+} was studied primarily in low phonon energy glass/fiber like tellurite glass, germanate glass, phosphate glass, fluoride glass, etc. due to their high quantum efficiency [6], [7]. However, considering stability of the silica glass and existing telecommunication system; modified silica host is more suitable and literatures are available dealing with amplification in the first telecommunication window around 0.8 μm [8], fiber amplifiers for S-band [9], [10], [11], and fiber laser at 2 μm [11], [12], [13]. In Tm-Yb doped silica glass, the quasi-resonant energy levels of Tm^{3+} with the excited Yb^{3+} level $^2F_{5/2}$ allow multistep $Yb^{3+} \longrightarrow Tm^{3+}$ energy transfer controlling the emission in the three major wavelength bands centering at 475, 800 and 2000 nm. Due to the non-resonant energy transfer, the possibility of the $Tm^{3+} \longrightarrow Yb^{3+}$ back-transfer is very low. However, proper selection of host glass composition, optimum dopant concentration, and appropriate Yb/Tm ratio are of paramount importance to achieve good lasing performance at NIR zone. However, as per our knowledge comparative study related to the effect of host glass composition suitable for NIR application is not described anywhere.

The present investigation is based on the above background and deals with the optimized fabrication parameters for Tm-Yb doped optical fiber (TY) based on different host glass compositions followed by their optical and material characterization results. The lasing performance of fiber samples and lifetimes are also compared, and possible reason of the observed result is presented.

2. Experimental

Tm-Yb doped optical fiber preform was fabricated through conventional modified chemical vapor deposition (MCVD) process [14], coupled with the solution

doping technique [15]. In order to compare fiber of different glass host, one need to have a set of constant fiber parameters namely numerical aperture (NA) and core diameter (necessary to match fiber cut-off value), Tm/Yb concentration level and their ratio which control the laser performance in final fiber. The fiber fabrication process comprises two main steps, namely preform fabrication and fiber drawing. The preform fabrication process starts with the deposition of the cladding layer composed of pure silica and the core layer containing silica soot doped with GeO_2 or P_2O_5 formed due to oxidation of reactant halide precursors ($SiCl_4$, $GeCl_4$, $POCl_3$) at appropriate temperature in presence of oxygen when heated externally by an oxy-hydrogen burner traversing along the tube length. The soot deposition temperature for the core layer deposition was precisely selected in order to achieve a uniform porous structure with good adhesion to the glass surface. The porous layer was then impregnated in an aqueous solution comprising different dopant ions, namely Tm, Yb and Al followed by subsequent processing to obtain a solid rod called the "perform". Acrylate polymer coated fiber, with bare fiber dimension of 125 ± 0.5 μm, was drawn from the fabricated preform in fiber drawing tower. The uniformity of refractive index profile (RIP) along the horizontal and the vertical direction of fabricated preform was measured using a preform analyser (PK2600, Photon Kinetics, USA) and fiber RIP using a NR-9200 fiber analyser (EXFO, Canada). The scanning electron microscope (SEM, LEO-s430-i) and high-resolution optical microscope (Olympus BX51) were used to investigate the characteristics of porous soot layers and to study the core-clad boundary nature. The distribution profiles of different dopants ions in the preform core were determined through electron probe microanalysis (EPMA) using a polished preform section of thickness 1.5 mm in an interval of 5 μm. The detail fabrication process can be found in previously published article [16]. The optimization of different fabrication parameters namely deposition of porous soot layer and solution impregnation are discussed in the following two paragraphs.

To examine the effect of host glass composition on the final fiber performance, preforms were fabricated selecting three different glass composition namely aluminosilicate glass (∼4.5wt % Al_2O_3), aluminogermano silicate glass (∼1wt % Al_2O_3 and 14wt % GeO_2) and alumino-phospho silicate glass (∼4wt % Al_2O_3 and 8wt % P_2O_5). Appreciable amount of Al-doping in each host glass was to ensure enhanced RE solubility [17] and to prevent unwanted clustering of RE ions. Since the porosity and the pore size distribution are two important parameters controlling dopant incorporation level and their overall distribution in the preform core; deposition temperature needs precise optimization. Accordingly, a series of preform runs were carried out with different host glass composition based on our selected vapor phase composition. The optimum deposition temperature for pure silica soot, GeO_2 - doped silica soot and P_2O_5 - doped silica soot, are found to be in the range of 1560 ± 10 °C, 1290 ± 10 °C and 1100 ± 10 °C respectively. The variation in the optimum deposition temperature for different host glass composition is a consequence of reduction in the silica glass viscosity with addition of dopants (GeO_2 and P_2O_5) and leads to partial sintering of the deposited soot layer [16]. During the deposition temperature optimization, precaution was taken to achieve good adhesion strength between the soot and glass surface to avoid peeling off the deposited soot layer during the solution impregnation stage. If the soot deposition temperature is higher than the optimum temperature, excess sintering of the soot layer will result in reduced dopant incorporation level with non-uniform dopant ion distribution, while at lower deposition temperature the soot layer peels off from the glass surface during solution impregnation stage. Other fabrication parameters namely tube rotation (80 rpm), burner traverse speed (125 mm/min) and bubbler temperature (25 °C) were kept fixed in different experiments.

Since the solution composition directly controls dopant incorporation level and solution viscosity, optimization of the solution composition was necessary which was achieved through varying concentration of $AlCl_3$, $6H_2O$ (99.9996 %, Alfa Aesar, Germany), $TmCl_3$, $6H_2O$ (99.99 %, Alfa Aesar, Germany) and $YbCl_3$, $6H_2O$ (99.99 %, Alfa Aesar, Germany) in different preform runs. Finally, to achieve Tm concentration in the range of 0.01–0.4 mol % with Yb to Tm ratio in the range of 1–2, the concentration of $YbCl_3$ salt was varied from 0.0075 to 0.15 M while for $TmCl_3$ the variation was from 0.008 to 0.04 M. The concentration of Al-salts was altered in the ranges of 0.3 to 1.25 M in different preform runs to maintain solution viscosities within 6-7 cP and to avoid Al-rich phase-separation during subsequent processing. Additionally, to achieve similar NA and fixed Yb to Tm ratio; the dipping period was adjusted in different preform runs within 30 to 60 minutes. Further, oxidation and dehydration condition was optimized to minimize the evaporation of dopant ions prior to sintering stage. We observed that, the dehydration temperature above 850 °C leads to evolution of strong red vapors and results in reduction of ∼80 ppm Tm-ions and accordingly the dehydration was carried out at around 800 °C. Our observation indicates that, beside dehydration temperature, dehydration time is also critical and need optimization to minimize the OH level to the maximum extent in order to avoid overlapping of Tm^{3+} ions absorption with OH absorption peak around 1.8 μm. The sintering of the soot layer was performed in a stepwise manner by increasing the burner temperature in an interval of 100 °C from 1000 to 1800 °C to prevent the phase separation and clustering of dopant ions within the preform

core region. To avoid the formation of the central dip in GeO_2-doped preform, "over doping" technique was adopted while collapsing by flowing measured quantity of $GeCl_4$.

Different properties such as absorption, emission cross-sections, lifetimes are important parameters to assess the laser and amplifier performance of a fiber and accordingly were evaluated prior to testing the lasing performance. The spectral attenuation measurement based on conventional cutback method was performed in Bentham set-up (UK made) to determine the attenuation of the fabricated fiber within the wavelength range of 350 to 2100 nm. The Ground State Absorption (GSA) was calculated using spectral attenuation data and the emission cross-section was evaluated employing McCumber equation [1] for different fabricated fibers. The Tm^{3+} and Yb^{3+} concentrations were additionally determined from the 785 nm ($^3H_6 \longrightarrow {}^3H_4$) and 975 nm ($^2F_{7/2} \longrightarrow {}^2F_{5/2}$) absorption peaks respectively and the values obtained were found to be in good agreement with the EPMA analysis.

The fiber performance such as saturated amplified spontaneous emission (ASE) spectrum around 2000 nm was measured by pumping the fabricated fiber at 980 nm when Yb^{3+} emission at 1060 nm helps in Tm^{3+} ions excitation to achieve pump saturation. The laser cavity was formed using an optimized length of TY fiber spliced with two FBGs at 1874 nm with reflectivities of 98 % and 38 %. A 980 nm laser diode possessing a maximum power of 480 mW was used as a pump source to obtain the maximum laser output power around 1599.05 nm [13]. During this experiment, an Er^{3+} doped fiber laser at ~1600 nm (developed by using 1.5 m of Er^{3+} doped fiber with Er^{3+} concentration ~5000 ppm) placed between two FBGs centered at 1599 nm with reflectivities of 99.4 % and 27.6 % was used as an auxiliary pump source, unidirectional with the 980 nm laser diode to excite the TY laser resonator. The power of the auxiliary pump at ~1600 nm was fixed at a minimum level to prevent the lasing at 1874 nm to utilize the 1600 nm pump only to excite the Tm^{3+} and not for power scaling.

3. Results & Discussion

Fabrication details, and fiber properties compared in this study are presented in Tab. 1. To avoid cross-relaxation process associated with a high level of Tm-ion concentration in doped fiber, we selected fiber samples containing Tm-ions in the range of 300 ppm to achieve efficient energy transfer from Yb to Tm ions.

RIP of the fabricated preform and the fibers are presented in Fig. 1a and Fig. 1b. Minimized central dip in RIP is achieved through fine optimization of fabrication parameters otherwise it is a common feature observed in the preform fabricated using the MCVD process, due to evaporation of oxide during the collapsing step specially in the case of GeO_2-doped preform/fiber.

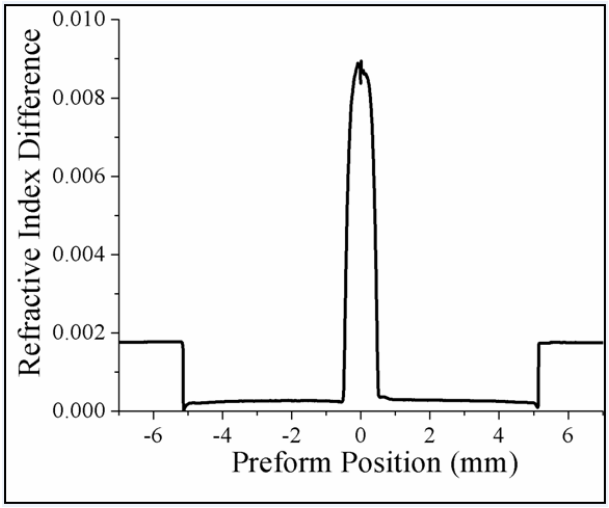

Fig. 1a: RIP of TY-2 preform.

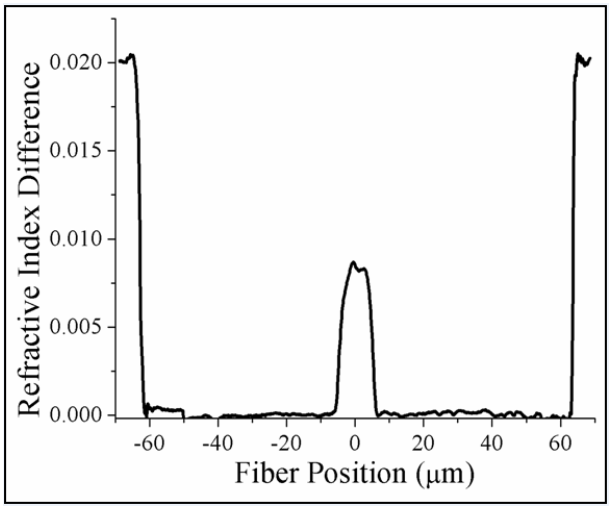

Fig. 1b: RIP of TY-2 fiber.

The dopant distribution profiles obtained from EPMA for TY-1, TY-2 and TY-3 are presented in Fig. 2a, Fig. 2b and Fig. 2c which exhibit uniform dopant distribution along the preform core. The small perturbation in Tm and Yb ion distribution along the preform core is common in the solution doping process. The amounts of incorporated Tm and Yb-ion concentration (in ppm) are almost similar and the ratio of Tm:Yb is around 1. Comparison of scanning electron microscopic images for the core-clad interface for the above three fiber samples revealed that alumino-silicate based fibers (TY-1) exhibit perfect core-clad interface while star-like growth is visible in the case of germano-alumino-silicate fibers (TY-2) as shown in Fig. 2d and Fig. 2e. The reason behind the origin of the core-clad

boundary problem in case of germano-alumino-silicate fiber sample is well studied and reported elsewhere [18].

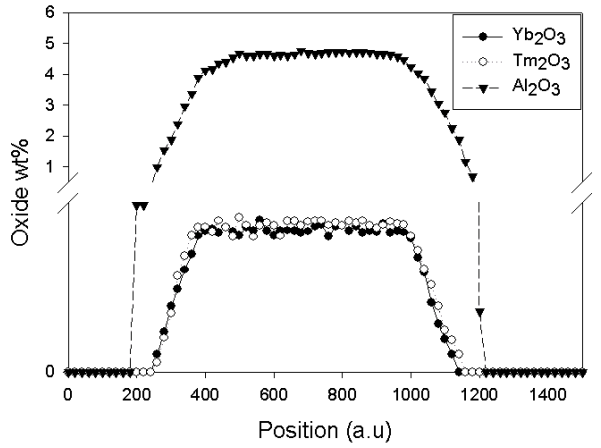

Fig. 2a: Tm-Yb distribution profiles in preform core of TY-1.

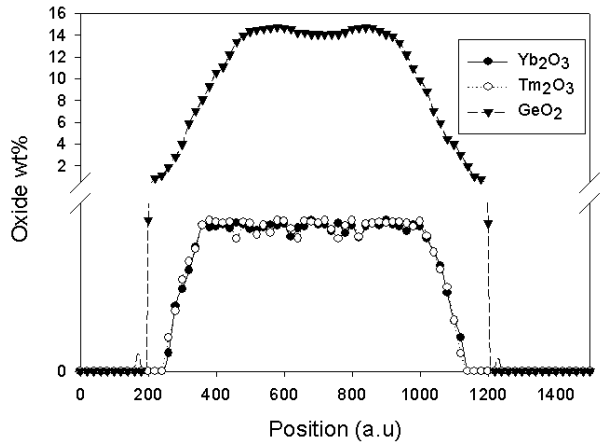

Fig. 2b: Tm-Yb distribution profiles in preform core of TY-2.

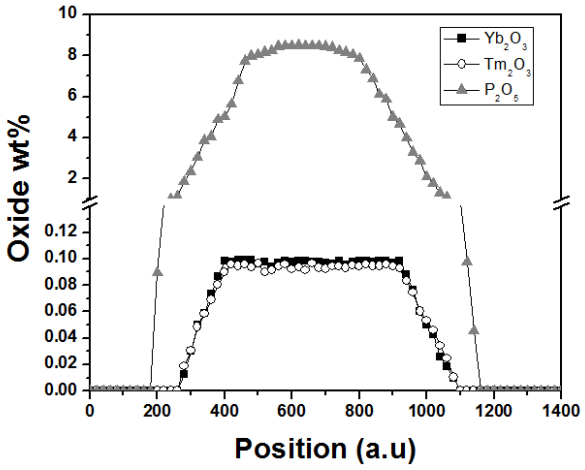

Fig. 2c: Tm-Yb distribution profiles in preform core of TY-3.

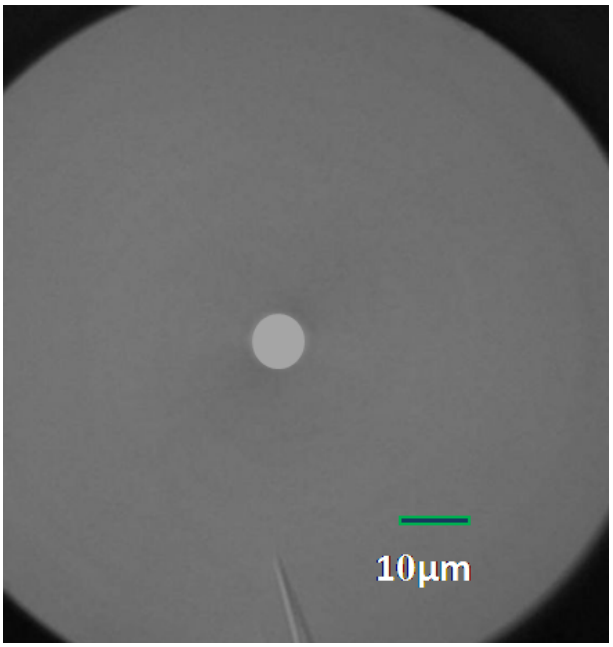

Fig. 2d: Optical microscopic view of core-clad interface of TY-1 fiber.

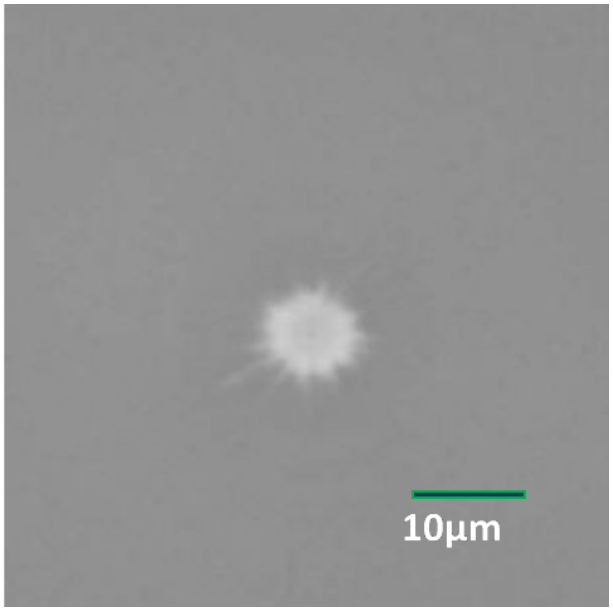

Fig. 2e: Optical microscopic view of core-clad interface of TY-2 fiber.

Ground state absorption spectra measured using conventional cut-back technique is presented in Fig. 3 which exhibit negligible OH level ($>$ 1 ppm) around 1240 and 1380 nm achieved due to optimized dehydration condition. Different peaks observed in Fig. 3 are centred at 750 nm ($^1G_4$-$^3H_6$), 800 nm ($^1G_4$-$^3H_6$), 975 nm ($^2F_{7/2}$-$^2F_{5/2}$), 1240 nm ($^3H_5$-$^3H_6$) and a broad peak around 1600 nm ($^3F_4$-$^3H_6$. The combined GSA spectra of three fiber samples normalized at 1600 nm presented in Fig. 4 indicate shifting of the 1600 nm peak due to change in host composition. The P_2O_5

Tab. 1: Details of representative preform runs.

ID	Vapor phase composition and deposition temperature	Core-Glass composition	Core:Clad [μm]	NA (±μm)	RE^{3+} concentration (± 15 ppm)		Tm/Yb ratio
					Tm	Yb	
TY-1	Pure SiO_2 1500 ± 5 °C	Al_2O_3-SiO_2-Yb_2O_3-Tm_2O_2	8.5:125	0.16	304	290	1
TY-2	Mol % SiO_2:GeO_2=0.86 1270 ± 5°C	Al_2O_3-GeO_2-SiO_2-Yb_2O_3 -Tm_2O_2	8.7:125	0.16	305	313	1
TY-3	Mol % SiO_2:P_2O_5=0.95 1050 ± 5°C	Al_2O_3-P_2O_5-SiO_2-Yb_2O_3-Tm_2O_2	8.5:125	0.16	309	317	1

doped fiber sample exhibits the red-shift while the GeO_2 doped fiber exhibits blue shifting. This peak shifting as a result of the host glass composition was already observed for Tm ions $^3H_4$ level and reported previously for S-band application [19]. Combined absorption and emission cross-section spectra in the wavelength range of 1400–2000 nm is also presented in Fig. 5 for TY-2 fiber [13].

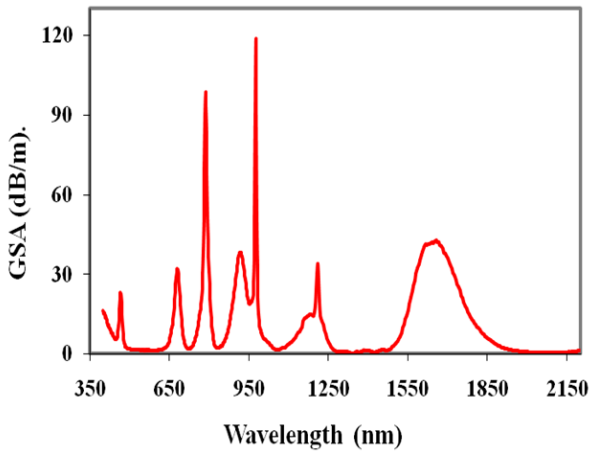

Fig. 3: Ground state absorption spectra of TY-2 fiber.

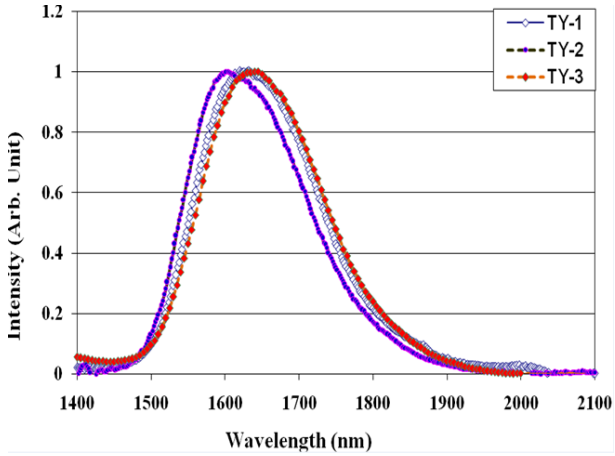

Fig. 4: Comparison of absorption spectra for three fibers at 1600 nm.

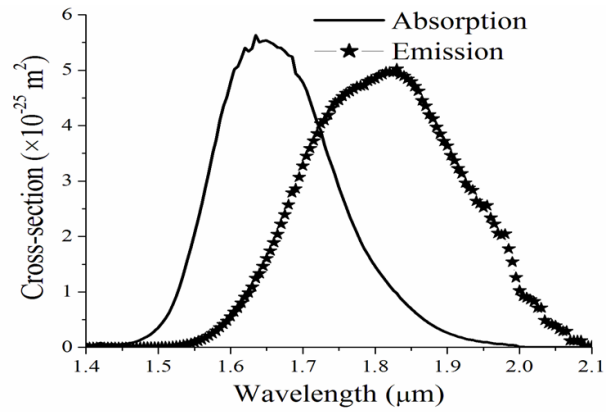

Fig. 5: Absorption and emission cross section of TY-2 fiber.

The radiative lifetime of $^3F_4$ level for Tm-ions was calculated based on the absorption and the emission cross-section peak line-width using Fuchtbauer-Ladenburg (FL) equation [20]. The result indicates that the GeO_2-doped system exhibits highest lifetime (7.1 ms) while the P_2O_5-doped system shows the least value (3.8 ms) with Al_2O_3-doped system exhibiting lifetime equal to 6.4 ms. Accordingly, it can be concluded that the probability of achieving the population inversion for $^3F_4$ level of Tm-ions necessary for the NIR lasing is easier for TY-2 fiber sample.

The amplified spontaneous emission (ASE) of three fibers were determined by pumping them using a 980 nm laser diode and analysis revealed that the P_2O_5-doped system produced a very weak ASE signal (not shown here) whereas the GeO_2-doped system exhibited higher and broader ASE signal. The experiment was conducted both for visible (980 nm) and NIR (2000 nm) region and the results are found to be similar and presented in Fig. 6a and Fig. 6b. To validate the obtained ASE result we compared the laser output power at 1874 nm with 980 and 1600 nm pump power. The experimental result revealed that both TY-1 and TY-2 exhibit good laser output power while TY-3 produced negligible power in the range of microwatt [not shown in Fig. 7a supporting our previous result. The combined result for achieved laser output power against the 980 nm pump powers is presented

in Fig. 7a [13] and for the 1600 nm pump in Fig. 7b below.

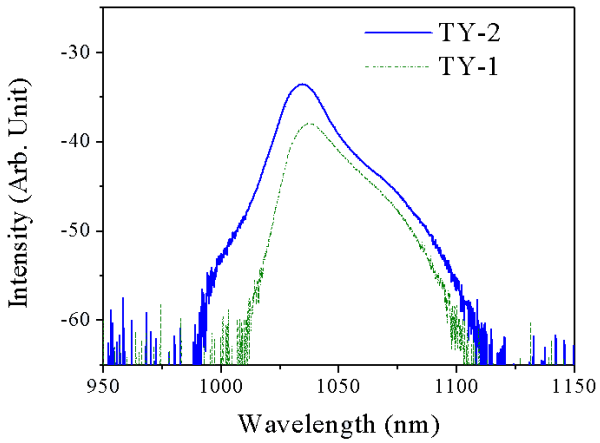

Fig. 6a: ASE curve for TY-1 and TY-2 fiber at 980 nm range.

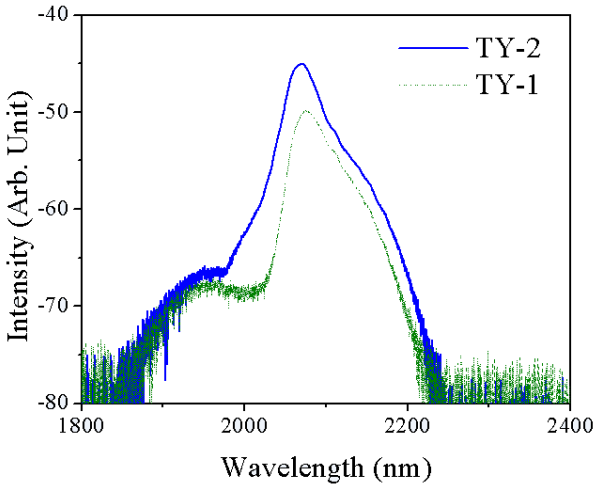

Fig. 6b: ASE curve for TY-1 and TY-2 fiber at 2000 nm range.

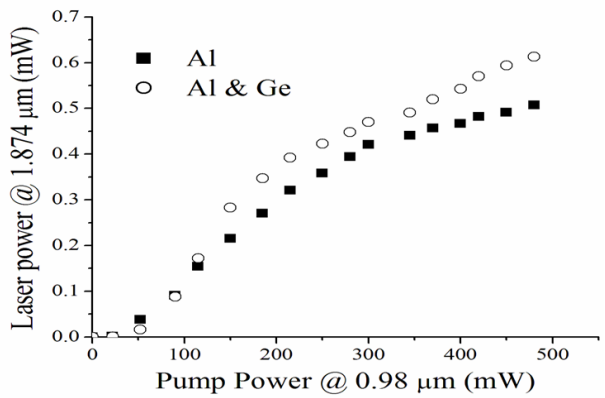

Fig. 7a: Comparison of laser performance at 980 nm.

All our observed results clearly indicate that both SiO_2 and SiO_2-GeO_2 doped with a suitable amount of Al_2O_3 are a better host compared to SiO_2-P_2O_5 doped

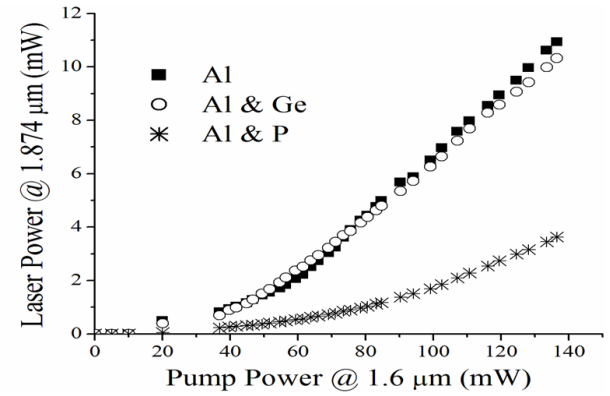

Fig. 7b: Comparison of laser performance at 1600 nm.

with Al_2O_3 under present investigation. The observation can be explained on the basis of phonon energy of the glass host under the investigation. Since, addition of dopants in pure silica alters the phonon energy of the glass; variations in the spectroscopic properties like lifetime and lasing performance are expected. Addition of phosphorous oxide in the silica glass enhances the phonon energy up to 1300 cm^{-1} and introduces high energy P=O bond which attracts more Tm ions towards itself and can lead to clustering of the Tm-ions. This problem is associated with the higher probability of non-radiative decay, non-homogeneous spectral broadening, reduced lasing performance and the quantum efficiency as evident from our result. On the contrary, GeO_2 and Al_2O_3 doping reduces the local phonon energy of the silica glass and consequently increase the $^3F_4$ level life result in time of the Tm^{3+} ion with additional benefit of achieving more homogeneous spectral broadening compared to the P_2O_5-doped glass. Between, TY-1 and TY-2, more significant change is expected in case of TY-1 and can be explained as follows. Ge is a four-coordinated network former and does not significantly alter the tetrahedral structure of the silica network. Additionally, the maximum phonon energy of the Ge-Si glass is about 1050 cm^{-1} which is close to pure silica [19] and thus has higher RE-clustering probability compared to Al_2O_3 doped glass system with the glass phonon energy around 800 cm^{-1}.

The observation that alumino-germano-silicate (TY-2) host provides better lasing and energy transfer performance compared to the alumino-silicate host fiber (TY-1) can be explained as follows. The GeO_2-doped glass sample contains a significant amount of Al_2O_3, however, the absolute Al-concentration is lower than that of TY-1. Although, in general Al doping expect to exhibits improved performance by increasing the lifetime (up to 3 times for $^3F_4$ and $^3H_4$ levels of Tm^{3+}) and thus the radiative transition of Tm^{3+} [2], but with the enhancement of the $^3F_4$ level lifetime, there is also significant enhancement in the $^3H_4$ lifetime. As per

our proposed configuration [13], a long $^3H_4$ lifetime will trigger the three-step energy transfer from $^3H_4$ to $^1G_4$. This will result in more enhanced blue emission ($^1G_4$ to $^3H_6$) and the radiative transition from $^3H_4$ to $^3H_6$, results in red emission. Accordingly, the energy transfer of the $^3F_4$ level from the $^3F_2$ level via the non-radiative transition of the $^3H_4$ level will reduce significantly. Since, the laser output in the NIR depends strongly on the population of the $^3F_4$ level, fiber TY-2 provides better laser output compared to TY-1.

4. Conclusion

The optimized fabrication of Tm-Yb doped fiber based on different host glass compositions namely pure silica, GeO_2-doped silica and P_2O_5-doped silica doped with Al_2O_3 has been described in detail, suitable for NIR application. Experimental result established that the GeO_2-doped silica containing the appropriate amount of Al_2O_3 exhibits best lasing performance in 2 μm region, while the P_2O_5-doped fiber does not exhibit any lasing performance at all. The observed result has been explained on the basis of the glass host composition based on their phonon energy. Further, improvement in the lasing performance can be achieved through fine tuning of the host glass composition by selection of suitable dopants to implement this fiber in 2 μm regions for sensing application.

Acknowledgment

The authors are pleased to acknowledge financial support of GLASSFIB project obtained from Council of Scientific and Industrial Research (CSIR), India.

References

[1] DIGONNET, M. J. *Rare-earth-doped fiber lasers and amplifiers*. 2nd ed. New York: Marcel Dekker, 2001. ISBN 08-247-0458-4.

[2] JACKSON, S. D. and T. A. KING. Theoretical modeling of Tm-doped silica fiber lasers. *Journal of Lightwave Technology*. 1999, vol. 17, iss. 5, pp. 948–956. ISSN 0733-8724. DOI: 10.1109/50.762916.

[3] SIMPSON, D. A. *Spectroscopy of Thulium Doped Silica Glass*. Victoria, 2008. Ph.D. thesis. Victoria University.

[4] FRIED, N. M, R. L. BLACKMON and B. P. IRBY. A review of thulium fiber laser ablation of kidney stones. In: *Proceedings of SPIE, Fiber Lasers VIII: Technology, Systems, and Applications (7914)*. San Francisco: Dawson, 2011. pp. 402–412. ISBN 9780819484512. DOI: 10.1117/12.878001.

[5] RICHARDS, B., S. SHEN and A. JHA. Spectroscopy of Tm-Ho co-doped tellurite glass for mid-IR fiber lasers in 1.8-2.2 μm. In: *Proceedings of SPIE, Lidar Technologies, Techniques, and Measurements for Atmospheric, Remote Sensing (5984)*. Bruges: SPIE, 2005. pp. 598407–598407–8. ISBN 0819460044. DOI: 10.1117/12.627838.

[6] SUN, H., L. ZHANGA, J. ZHANG, L. WEN, C. YU, Z. DUAN, S. DAI, L. HU and Z. JIANG. Intense upconversion luminescence in ytterbium-sensitized thulium-doped oxychloride germanate glass. *Physica B: Condensed Matter*. 2005, vol. 358, iss. 1–4, pp. 50–55. ISSN 0921-4526. DOI: 10.1016/j.physb.2004.12.025.

[7] RICHARDS, B., S. SHEN, A. JHA, Y. TSANG and D. BINKS. Infrared emission and energy transfer in Tm^{3+}, Tm^{3+}-Ho^{3+} and Tm^{3+}-Yb^{3+}-doped tellurite fiber. *Optics Express*. 2007, vol. 15, iss. 11, pp. 6546–6551. ISSN 1094-4087. DOI: 10.1364/OE.15.006546.

[8] WATEKAR, P. R., J. SEONGMIN and H. WON-TAEK. 800-nm upconversion emission in Yb-sensitized Tm-doped optical fiber. *IEEE Photonics Technology Letters*. 2006, vol. 18, iss. 15, pp. 1609–1611. ISSN 1041-1135. DOI: 10.1109/LPT.2006.879584.

[9] CHANG, J., Q.-P. WANG and G.-D. PENG. Optical amplification in Yb3 -codoped thulium doped silica fiber. *Optical Materials*. 2006, vol. 28, iss. 8–9, pp. 1088–1094. ISSN 0925-3467. DOI: 10.1016/j.optmat.2005.06.015.

[10] KOZAK, M. M., R. CASPARY and W. KOWALSKY. Thulium-doped fiber amplifier for the S-band. In: *Proceedings of 2004 6th International Conference on Transparent Optical Networks*. Wroclaw: IEEE, 2004, pp. 51–54. ISBN 0-7803-8343-5. DOI: 10.1109/ICTON.2004.1361967.

[11] JACKSON, S. D. Power scaling method for 2-μm diode-cladding-pumped Tm^3-doped silica fiber lasers that uses Yb^3 codoping. *Optics Letters*. 2003, vol. 28, iss. 22, pp. 2192–2194. ISSN 1539-4794. DOI: 10.1364/OL.28.002192.

[12] JEONG, Y., P. DUPRIEZ, J. K. SAHU, J. NILSSON and D. SHEN, A. W. CLARKSON and S. D. JACKSON. Thulium-ytterbium co-doped fiber laser with 75W of output power at 2 microns. In:

Proceedings of SPIE, solid State Laser Technologies and Femtosecond Phenomena (5620). London: SPIE, 2004, pp. 1–8. ISBN 9780819455734. DOI: 10.1117/12.578727

[13] PAL, A., A. DHAR, S. DAS, S. Y. CHEN, T. SUN, R. SEN and K. T. V. GRATTAN. Ytterbium-sensitized Thulium-doped fiber laser in the near-IR with 980 nm pumping. *Optics Express*. 2010, vol. 18, iss. 5, pp. 5068–5074. ISSN 1094-4087. DOI: 10.1364/OE.18.005068.

[14] NAGEL, S. R., J. B. MACCHESNEY and K. L. WALKER. An Overview of the Modified Chemical Vapor Deposition (MCVD) Process and Performance. *IEEE Transactions on Microwave Theory and Techniques*. 1982, vol. 30, iss. 4, pp. 305–322. ISSN 0018-9197. DOI: 10.1109/TMTT.1982.1131071.

[15] TOWNSEND, J. E., S. B. POOLE and D. N. PAYNE. Solution-doping technique for fabrication of rare-earth-doped optical fibres. *Electronics Letters*. 1987, vol. 23, iss. 7, pp. 329–331. ISSN 1350-911X. DOI: 10.1049/el:19870244.

[16] DHAR, A., M. PAUL, M. PAL, A. K. MONDAL, S. SEN, H. S. MAITI and R. SEN. Characterization of porous core layer for controlling rare earth incorporation in optical fiber. *Optics Express*. 2006, vol. 14, iss. 20, pp. 9006–9015. ISSN 1094-4087. DOI: 10.1364/OE.14.009006.

[17] MACDOWELL, J. F. and G. H. BEALL. Immiscibility and Crystallization in $A1_2O_2$-SiO_2 Glasses. *Journal of the American Ceramic Society*. 1969, vol. 52, iss. 1, pp. 17–25. ISSN 1551-2916. DOI: 10.1111/j.1151-2916.1969.tb12653.x.

[18] DHAR, A., S. DAS, H. S. MAITI and R. SEN. Fabrication of high aluminium containing rare-earth doped fiber without core–clad interface defects. *Optics Communications*. 2010, vol. 283, iss. 11, pp. 2344–2349. ISSN 0030-4018. DOI: 10.1016/j.optcom.2010.02.001.

[19] FAURE, B., W. BLANC, B. DUSSARDIER and G. MONNOM. Improvement of the Tm^{3+}:$^3H_4$ level lifetime in silica optical fibers by lowering the local phonon energy. *Journal of Non-Crystalline Solids*. 2007, vol. 353, iss. 29, pp. 2767–2773. ISSN 0022-3093. DOI: 10.1016/j.jnoncrysol.2007.05.025.

[20] TACCHEO, S., P. LAPORTA, S. LONGHI, O. SVELTO and C. SVELTO. Diode-pumped bulk erbium-ytterbium lasers. *Applied Physics B Laser and Optics*. 1996, vol. 63, iss. 5, pp. 425–436. ISSN 0946-2171. DOI: 10.1007/BF01828937.

About Authors

Anirban DHAR was born in 1977 Kolkata, India. He received his M.Sc. from University of Calcutta in 2001 and Ph.D. from Jadavpur University, India in 2008. He joined CSIR-CGCRI in 2012 as Scientist. His research interests include fabrication and characterization of specialty optical fiber for amplifier, laser and sensor application.

Atasi PAL received her Bachelor of Engineering degree in Electronics & Telecommunication from Jadavpur University, Kolkata, India in 2003 and Ph.D. in Electrical Engineering from City University London, UK in 2013. She joined CSIR-CGCRI, Kolkata, India, in 2004 where she is currently working as Scientist. Her research interest focuses on the design and characterization of specialty optical fiber and fiber laser for medical application and sensing.

Shyamal DAS received the B.E, M.E degrees in Chemical Engineering and Ph.D. (Engg.) degree in the field of sol-gel processing from Jadavpur University. Presently, he is working as a Scientist in Fiber optics and photonics division of CSIR-CGCRI where he joined in 2006. His research interests include fabrication of erbium-doped fiber, large flattened mode fiber, thulium doped fiber and specialty optical fiber.

Ranjan SEN received his B.E, M.E in Chemical Engineering and Ph.D. in Engineering from Jadavpur University. He is presently head of Glass Division and Chief Scientist of Fiber Optics and Photonics Division, CSIR-CGCRI. His research interest includes Specialty optical fibers for applications in high power fiber laser, Optical amplifier, fiber Bragg gratings, interferrometric sensors etc. In the area of Glass Science and technology, the research interest is primarily towards specialty glass and glass ceramics for advanced applications.